

Impact of the PDFs on the determination of MW with a specific attention to bin-bin correlations

Emanuele A. Bagnaschi (PSI)

PAUL SCHERRER INSTITUT



07 February 2019

Kick-off meeting of the PRIN “Precision electroweak physics at the CERN Large Hadron Collider”

Pisa, Italy

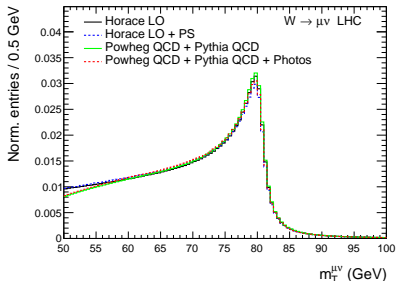
Introduction and motivations

Introduction and motivations

- Study the role of bin-bin correlations in the procedure used to estimate/include PDF uncertainty in the extraction of M_W at the LHC, with a specific focus on the long term perspectives.
- Three sets of uncertainties linked to PDFs:
 1. **Uncertainty in the PDFs from the experimental uncertainty of the dataset used in the fit.**
 2. Different fit methodologies (i.e. differences between PDF sets of different collaborations).
 3. Theoretical uncertainties of the predictions used in PDF fits. Concerning Missing Higher Order Uncertainties (MHOUs), their inclusion is starting to be addressed systematically only recently ([L. A. Harland-Lang, R. S. Thorne – 1811.08434], [R. A. Khalek et al. (NNPDF) – 1906.10698]).

Measuring the W mass at the LHC

Three observables sensitive to the W mass: M_T^W , p_{\perp}^l , $p_T(\text{missing})$.



- Peak around m_W .
- $M_T = \sqrt{2p_T^l p_T^{\text{miss}}(1 - \cos \Delta\phi)}$
- Suffer from pileup and detector effects since it relies on \vec{E}_T .
- Stability under QCD radiative corrections.

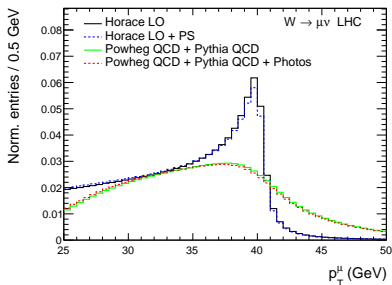
[Carloni Calame et al '16]

W-boson charge Kinematic distribution	W^+		W^-		Combined	
	p_T^l	m_T	p_T^l	m_T	p_T^l	m_T
δm_W [MeV]						
$\langle \mu \rangle$ scale factor	0.2	1.0	0.2	1.0	0.2	1.0
$\Sigma \vec{E}_T$ correction	0.9	12.2	1.1	10.2	1.0	11.2
Residual corrections (statistics)	2.0	2.7	2.0	2.7	2.0	2.7
Residual corrections (interpolation)	1.4	3.1	1.4	3.1	1.4	3.1
Residual corrections ($Z \rightarrow W$ extrapolation)	0.2	5.8	0.2	4.3	0.2	5.1
Total	2.6	14.2	2.7	11.8	2.6	13.0

[ATLAS 1701.07240]

Measuring the W mass at the LHC

Three observables sensitive to the W mass: M_T^W , p_{\perp}^l , $p_T(\text{missing})$.



- Peak around $m_W/2$.
- Detector modeling under control.
- High sensitivity to radiative corrections.
- We focus on p_{\perp}^l .

[Carloni Calame et al '16]

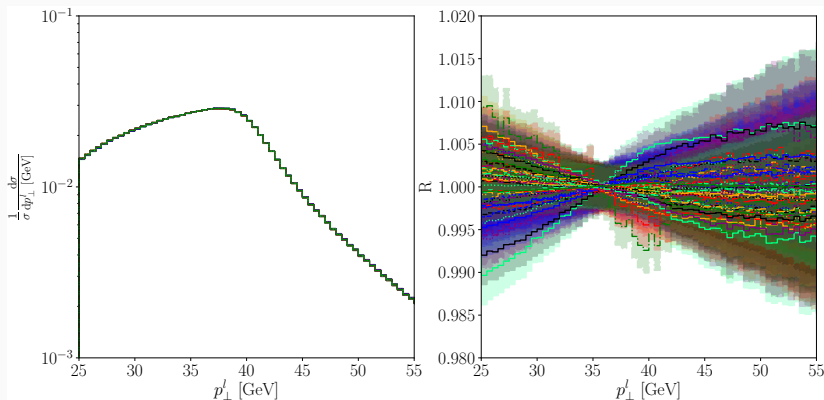
W-boson charge Kinematic distribution	W^+		W^-		Combined	
	p_{\perp}^l	m_T	p_{\perp}^l	m_T	p_{\perp}^l	m_T
δm_W [MeV]						
$\langle \mu \rangle$ scale factor	0.2	1.0	0.2	1.0	0.2	1.0
ΣE_T correction	0.9	12.2	1.1	10.2	1.0	11.2
Residual corrections (statistics)	2.0	2.7	2.0	2.7	2.0	2.7
Residual corrections (interpolation)	1.4	3.1	1.4	3.1	1.4	3.1
Residual corrections ($Z \rightarrow W$ extrapolation)	0.2	5.8	0.2	4.3	0.2	5.1
Total	2.6	14.2	2.7	11.8	2.6	13.0

[ATLAS 1701.07240]

The study

Monte-Carlo setup

- W^+ generated with POWHEG-BOX-v2 W_ew-BMNNP, $\sqrt{S} = 13$ TeV, $\mu_r = \mu_f = m_W$.
- Accuracy: NLO-QCD+PS, showered with PYTHIA82.
- Cuts: $|\eta_l| < 2.5$, $p_l > 25$ GeV, $\cancel{E}_T > 25$ GeV.
- 15 million events; reweighted to the full set of 1000 replicas of NNPDF30-1000.



Previous studies for M_W

- Tevatron collaborations [0707.0085,0708.3642,0908.0766,1203.0275,1203.0293,1307.7627].
- Comprehensive study on the PDF uncertainty on M_T^W using modern matched MCs (see also [Bozzi, Rojo, Vicini – 1104.2056]), however with inaccurate M_T^W modeling.
- Subsequent study on p_T^l presented in [Bozzi, Citelli, Vicini – 1501.05587] and extended to the study of a high-rapidity lepton in [Bozzi, Citelli, Vesterinen, Vicini – 1508.06954].

Prescription for the estimation of the uncertainty in those studies

- Generate M_W -templates using the central replica of the NNPDF set.
 - $\chi_{k,r}^2 = \sum_{i \in bins} (\mathcal{T}_{0,k} - \mathcal{D}_r)_i^2 / \sigma_i^2$.
 - Fit other NNPDF replica; compute the standard deviation of the M_W corresponding to minima of the replica χ^2 and take it as a proxy of the PDF uncertainty.
 - Neglect the value of the χ^2 .
 - Fixed fit range, $p_{\perp}^l \in [29, 49]$ GeV.
-
- ATLAS [1701.07240], [Kotwal PRD 98, 033008].
 - Other recent studies: [E. Manca, O. Cerri, N. Foppiani, L. Rolandi – 1707.09344], [L. Bianchini and G. Rolandi – 1902.03028], [S. Farry, O. Lupton, M. Pili, M. Vesterinen – 1902.04323], [M. Hussein, J. Isaacson, J. Huston – 1905.00110].

The role of bin-bin PDF correlations

Experimental side

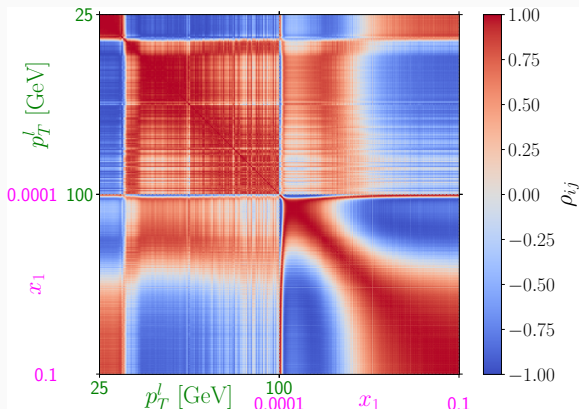
- They were *not* included in the published M_W measurement from ATLAS, though the effect has been partially included through the combination of different categories.
- They will be included in future measurements both from ATLAS and CMS.
- They were included in other measurements (e.g. $\sin^2 \theta_1^{eff}$, or α_s).

Phenomenological studies

- Included in the recent [S. Farry, O. Lupton, M. Pili, M. Vesterinen – 1902.04323], through a Bayesian reweighting procedure.

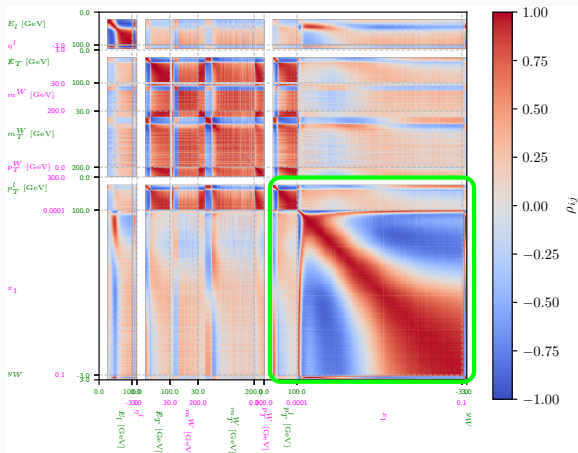
- What is the structure and origin of the bin-bin p_T^l correlations?
- What is the perspective for a measurement with a large integrated luminosity?

p_{\perp}^l and PDF correlations



- Different elements drive correlation between replicae (QCD framework)
- $(\Sigma_{PDF})_{rs} = \langle (\mathcal{T} - \langle \mathcal{T} \rangle_{PDF})_r (\mathcal{T} - \langle \mathcal{T} \rangle_{PDF})_s \rangle_{PDF}$
- Block-structure in the p_{\perp}^l self-correlation (top-left corner).
- Interplay in the hadron level cross-section between the parton-level cross-section and the luminosity.

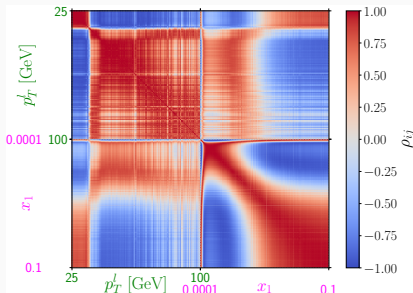
Other observables



(caveat: *only* this plot at NNPDF30-100/LHEF)

- Shapes of differential observables non-trivially correlated under PDF variation

Fitting methodology



- Fit the (pseudo)data using the templates (in our case the central replica in both cases), introducing a covariance matrix in the χ^2 definition.
- Estimate the PDF uncertainty as the half-width of the $\Delta\chi^2 = 1, 4, 9$ interval.
- The covariance matrix shows a non-trivial structure that has an impact in reducing the sensitivity to the PDF in the fit.

$$\chi_{k,min}^2 = \sum_{(r,s) \in bins} (\mathcal{T}_{0,k} - \mathcal{D}^{exp})_r (\mathbf{C}^{-1})_{rs} (\mathcal{T}_{0,k} - \mathcal{D}^{exp})_s$$

$$\mathbf{C} = \Sigma_{PDF} + \Sigma_{stat} + \Sigma_{MC} + \Sigma_{exp, syst}$$

$$(\Sigma_{PDF})_{rs} =$$

$$\langle (\mathcal{T} - \langle \mathcal{T} \rangle_{PDF})_r (\mathcal{T} - \langle \mathcal{T} \rangle_{PDF})_s \rangle_{PDF}$$

$$\langle \mathcal{O} \rangle_{PDF} \equiv \frac{1}{N_{cov}} \sum_{l=1}^{N_{cov}} \mathcal{O}^{(l)}$$

Results

Numerical results: without any covariance

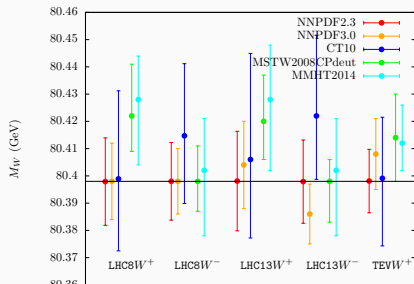
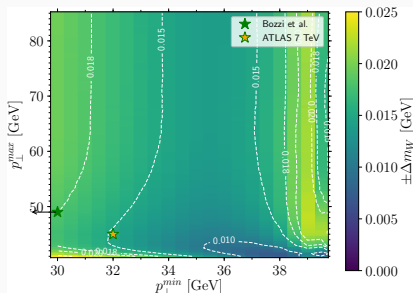


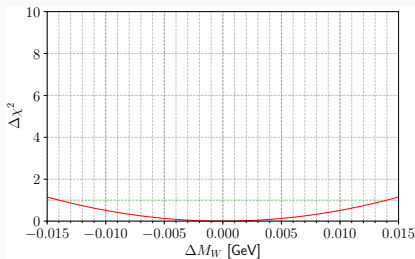
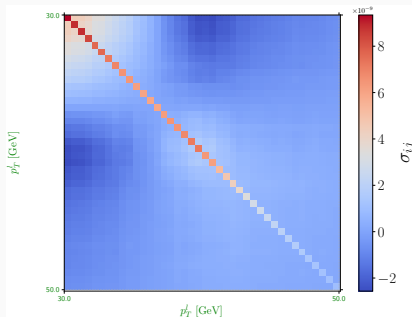
Fig. 4 left from [BCV - 1501.05587]



- $\chi_{k,r}^2 = \sum_{i \in bins} (\mathcal{T}_{0,k} - \mathcal{D}_r)_i^2 / \sigma_i^2$.
- Compatible results for (nearly) the same fit window.
- The study shows a sizable variability on the fit range.

Numerical results: with stat+PDF covariance

- PDF covariance + 1fb^{-1} stat. included.

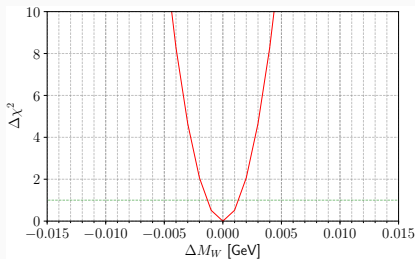
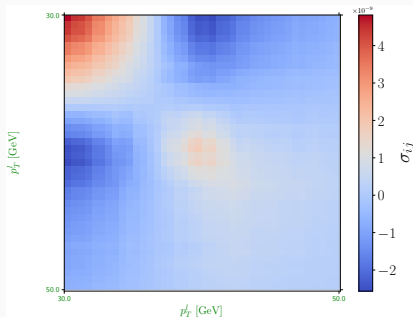


$$\chi_{k,min}^2 = \sum_{(r,s) \in bins} (\mathcal{T}_{0,k} - \mathcal{D}^{exp})_r \left(C^{-1} \right)_{rs} (\mathcal{T}_{0,k} - \mathcal{D}^{exp})_s$$

$$C = \Sigma_{PDF} + \Sigma_{stat}$$

Numerical results: with stat+PDF covariance

- PDF covariance + 300fb^{-1} stat. included.

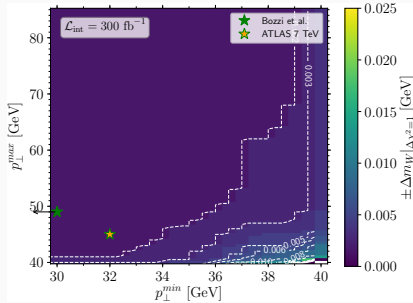
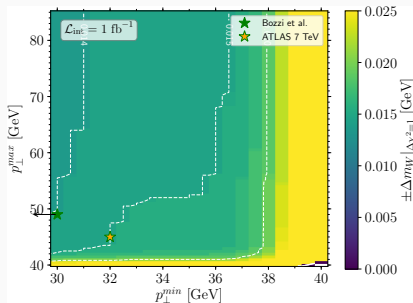


$$\chi_{k,min}^2 = \sum_{(r,s) \in bins} (\mathcal{T}_{0,k} - \mathcal{D}^{exp})_r \left(C^{-1} \right)_{rs} (\mathcal{T}_{0,k} - \mathcal{D}^{exp})_s$$

$$C = \Sigma_{PDF} + \Sigma_{stat}$$

Numerical results: with MC+stat+PDF covariance

- No MC uncertainty.
- Add MC uncertainty corresponding to 10^{10} events.



- Large statistics is needed but it does not seem a limiting factor.
-

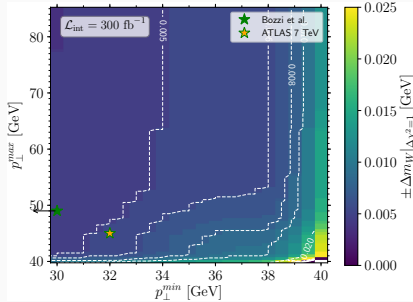
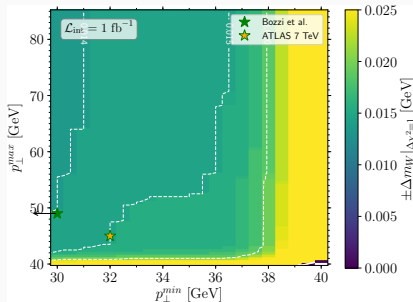
$$\chi_{k,min}^2 = \sum_{(r,s) \in bins} (\mathcal{T}_{0,k} - \mathcal{D}^{exp})_r \left(\mathbf{C}^{-1} \right)_{rs} (\mathcal{T}_{0,k} - \mathcal{D}^{exp})_s$$

$$\mathbf{C} = \Sigma_{PDF} + \Sigma_{stat} + \Sigma_{MC}$$

- What about other source of uncertainties?

Numerical results: with MC+stat+PDF covariance

- No MC uncertainty.
- Add MC uncertainty corresponding to 10^{10} events.



- Large statistics is needed but it does not seem a limiting factor.
-

$$\chi_{k,min}^2 = \sum_{(r,s) \in bins} (\mathcal{T}_{0,k} - \mathcal{D}^{exp})_r \left(\mathbf{C}^{-1} \right)_{rs} (\mathcal{T}_{0,k} - \mathcal{D}^{exp})_s$$

$$\mathbf{C} = \Sigma_{PDF} + \Sigma_{stat} + \Sigma_{MC}$$

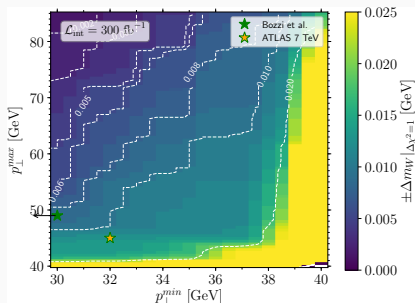
- What about other source of uncertainties?

Numerical results: with sys+stat+PDF covariance

- We tried to qualitative understand the impact of detector effects on p_{\perp}^j .
- We used the model proposed by E. Manca (CMS) [[CERN-THESIS-2016-173](#)].

$$\left(\frac{\sigma_{p_T^j}}{p_T^j}\right)^2 = a^2(\eta_l) \cdot r_L^2(\eta_l) + c^2(\eta_l) p^2 \cdot r_L^4(\eta_l) + \frac{b^2(\eta_l) \cdot r_L^2(\eta_l)}{1 + \frac{d^2(\eta_l)}{p^2} \cdot \frac{1}{r_L^2(\eta_l)}}$$

- Uncertainty of 10^{-4} GeV on the overall muon scale.



- We compute a “CMS-covariance matrix” using 100 toys. We sum it to the PDF+stat covariance matrix.
- Detector effects reduce the efficacy of the method.
- A quantitative precise statement on the PDF uncertainty depends on the details of the all the systematics of the measurements.

Conclusions and outlook

Conclusions and outlook

Summary

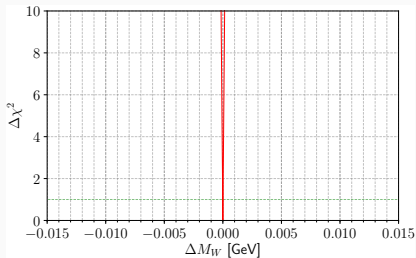
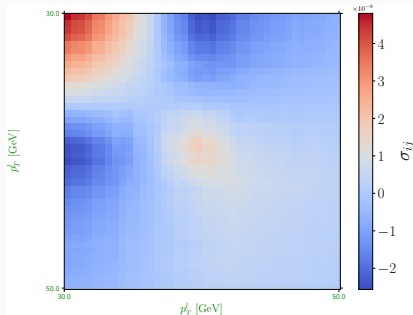
- Treat PDF uncertainty in a frequentist framework as nuisances \rightarrow covariance matrix.
- Correlation structure of bin above/below the Jacobian peak non-trivial.
- Fitting including the full covariance matrix shows a reduced sensitivity to the PDF uncertainty, if other source of errors are under control.
- Inclusion of bin-bin correlations especially beneficial with large integrated luminosity and good control over the systematics.

Future developments

- What happens to the correlations if we fix the PDF methodology but we change data sets? Disentangle theory vs experimental effects.
- Correlation structure in the other (Hessian) PDF sets.
- Differences between different sets.
- Scale/smearing/MC-modelling dependence of the covariance matrix?

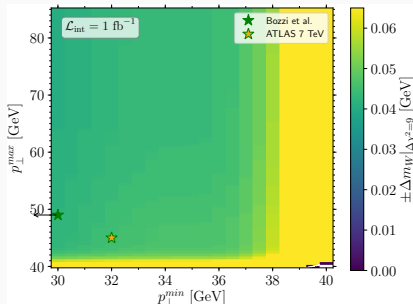
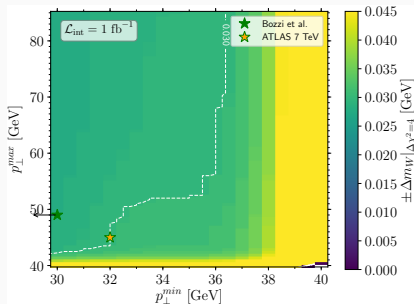
Backup slides

Numerical results: with PDF covariance



- Shape fit in $p_{\perp}' \in [30, 50]$ GeV.
- Only PDF covariance included.

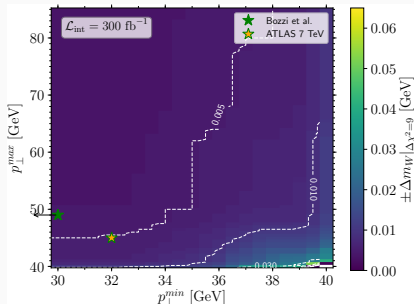
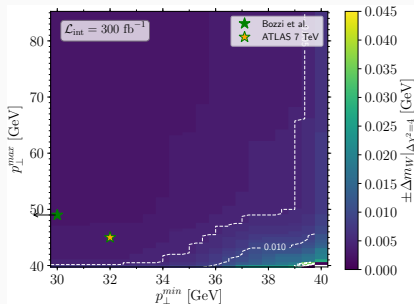
$\mathcal{L}_{\text{int}} = 1 \text{ fb}^{-1}$, 2σ and 3σ intervals



- $\Delta \chi^2 = 4$ half-interval.

- $\Delta \chi^2 = 9$ half-interval.

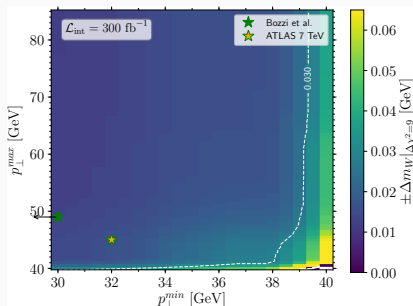
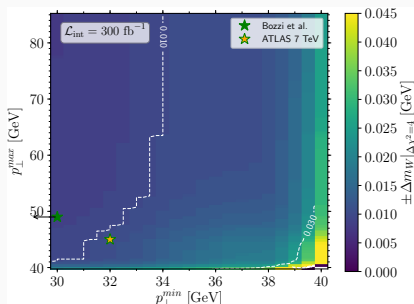
$\mathcal{L}_{\text{int}} = 300 \text{ fb}^{-1}$, 2σ and 3σ intervals



- $\Delta \chi^2 = 4$ half-interval.

- $\Delta \chi^2 = 9$ half-interval.

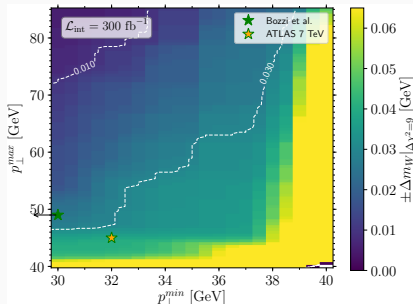
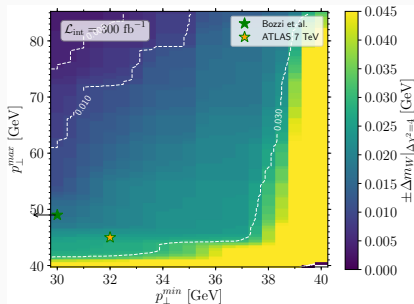
$\mathcal{L}_{\text{int}} = 300 \text{ fb}^{-1} + \text{MC } 10^{10} \text{ events, } 2 \sigma / 3 \sigma \text{ intervals}$



- $\Delta \chi^2 = 4$ half-interval.

- $\Delta \chi^2 = 9$ half-interval.

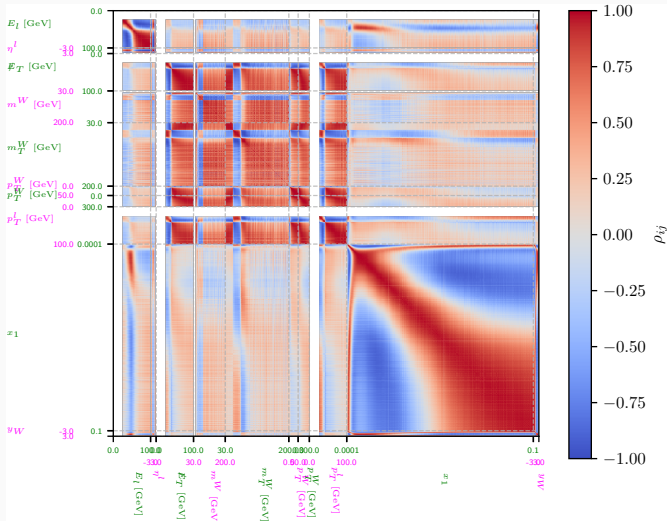
$\mathcal{L}_{\text{int}} = 300 \text{ fb}^{-1} + \text{smearing } 2 \sigma \text{ and } 3 \sigma \text{ intervals}$



- $\Delta\chi^2 = 4$ half-interval.

- $\Delta\chi^2 = 9$ half-interval.

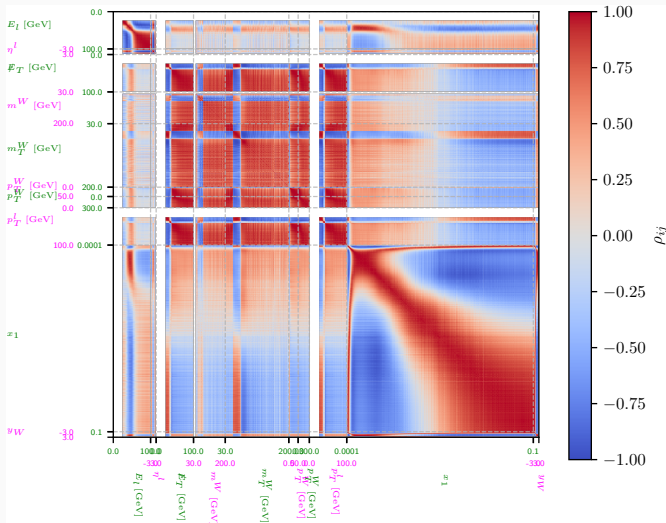
Bin-bin PDF correlation and partonic channels



- all-channels

(caveat: this plot at
NNPDF30-100/LHEF)

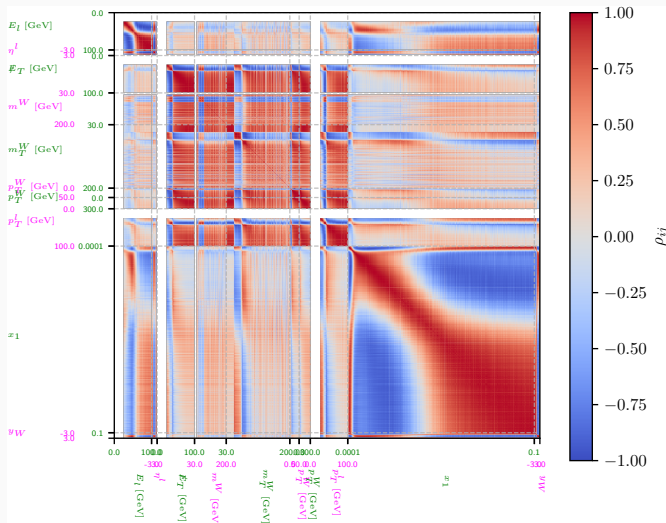
Bin-bin PDF correlation and partonic channels



- qq'-channels

(caveat: this plot at
NNPDF30-100/LHEF)

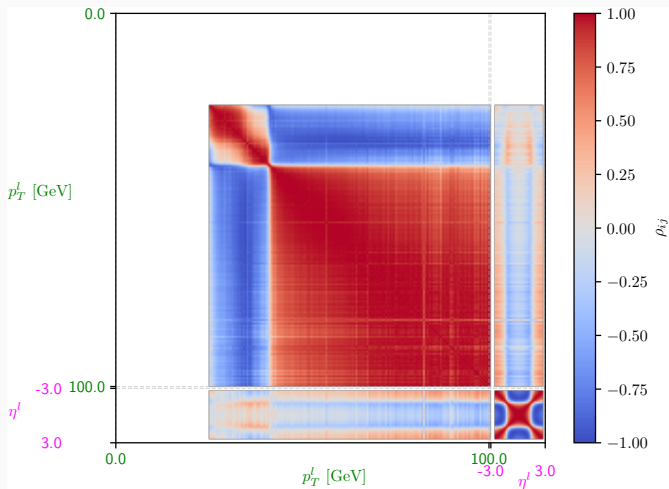
Bin-bin PDF correlation and partonic channels



- qg-channels

(caveat: this plot at
NNPDF30-100/LHEF)

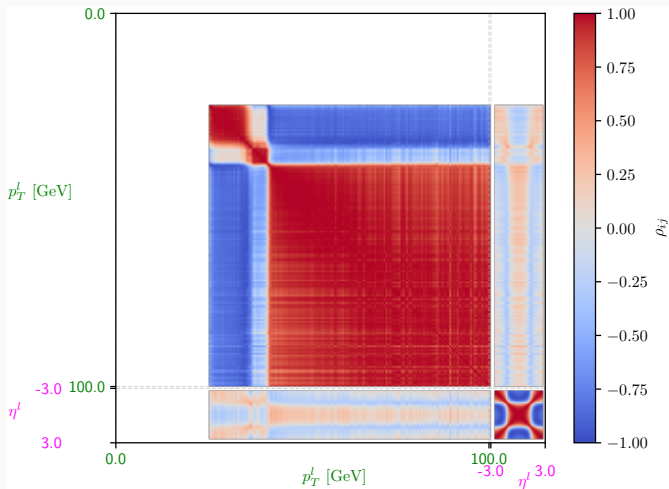
$p_T^l - \eta_l$ correlation



■ all-channels

(caveat: this plot at
NNPDF30-100/LHEF)

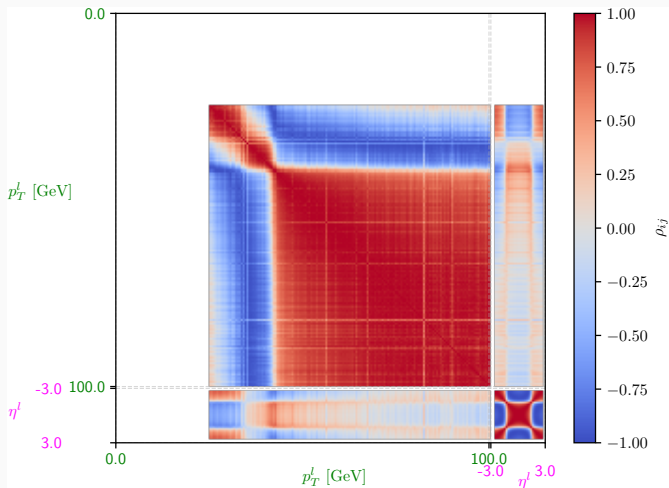
$p_T^l - \eta_l$ correlation



- qq'-channels

(caveat: this plot at
NNPDF30-100/LHEF)

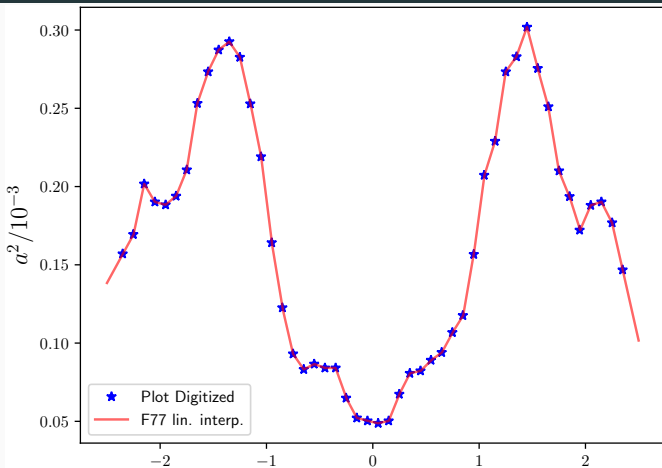
$p_T^l - \eta_l$ correlation



- qg-channels

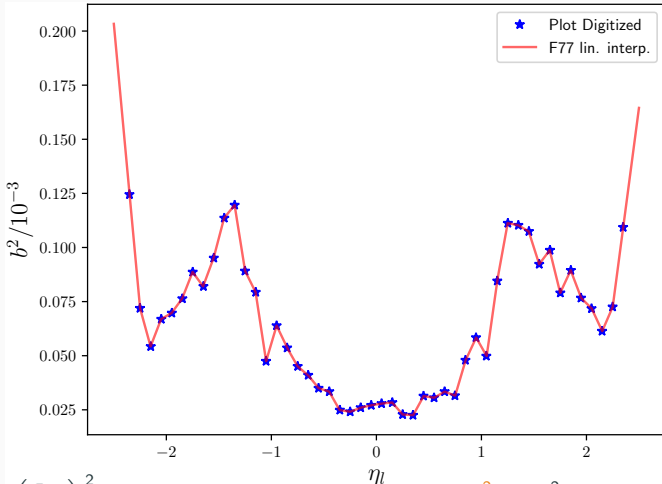
(caveat: this plot at
NNPDF30-100/LHEF)

p'_\perp smearing



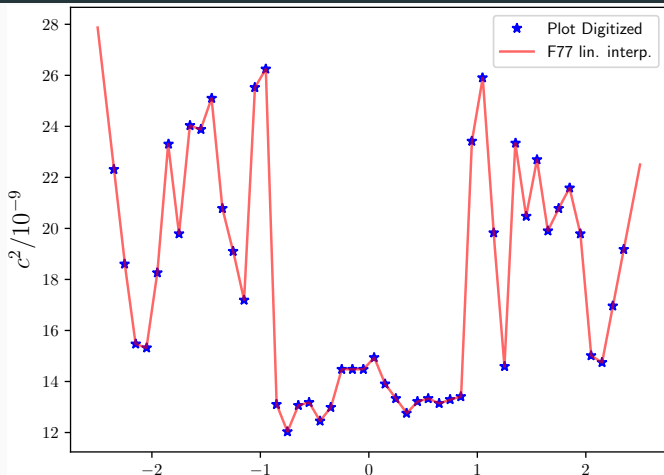
$$\left(\frac{\sigma_{p'_T}}{p'_T}\right)^2 = a^2(\eta_l) \cdot r_L^2(\eta_l) + c^2(\eta_l) p_T^2 \cdot r_L^4(\eta_l) + \frac{b^2(\eta_l) \cdot r_L^2(\eta_l)}{1 + \frac{d^2(\eta_l)}{p^2} \cdot \frac{1}{r_L^2(\eta_l)}}$$

p'_\perp smearing



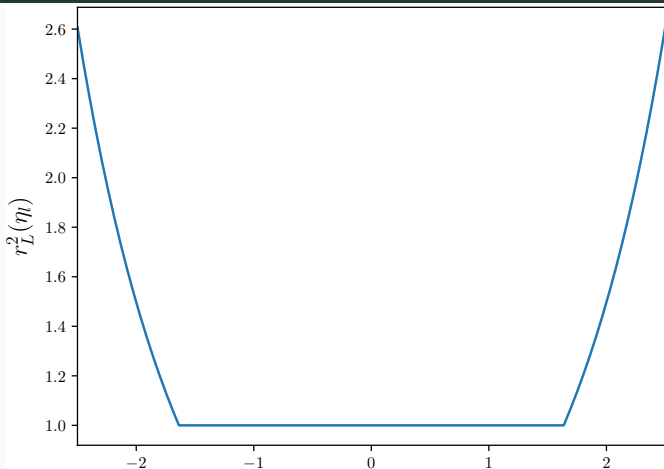
$$\left(\frac{\sigma_{p'_T}}{p'_T}\right)^2 = a^2(\eta_l) \cdot r_L^2(\eta_l) + c^2(\eta_l) p_T^2 \cdot r_L^4(\eta_l) + \frac{b^2(\eta_l) \cdot r_L^2(\eta_l)}{1 + \frac{d^2(\eta_l)}{p^2} \cdot \frac{1}{r_L^2(\eta_l)}}$$

p'_\perp smearing



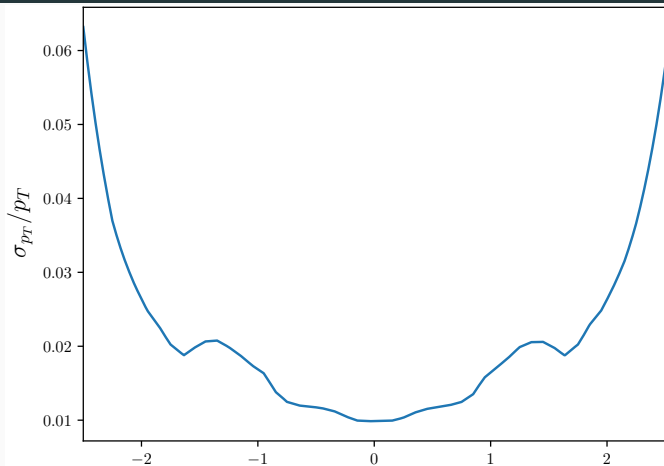
$$\left(\frac{\sigma_{p'_T}}{p'_T}\right)^2 = a^2(\eta_l) \cdot r_L^2(\eta_l) + c^2(\eta_l) p_T^2 \cdot r_L^4(\eta_l) + \frac{b^2(\eta_l) \cdot r_L^2(\eta_l)}{1 + \frac{d^2(\eta_l)}{p^2} \cdot \frac{1}{r_L^2(\eta_l)}}$$

p'_\perp smearing



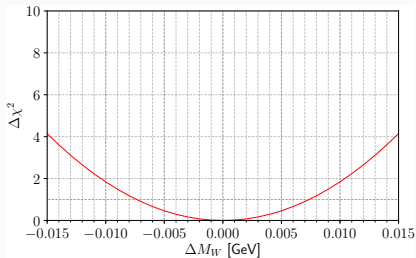
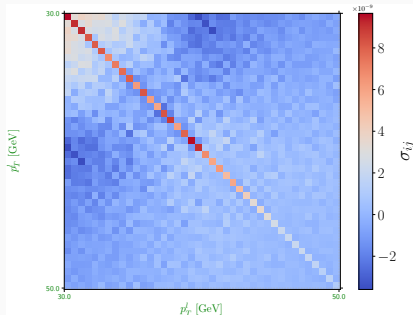
$$\left(\frac{\sigma_{p'_T}}{p'_T}\right)^2 = a^2(\eta) \cdot r_L^2(\eta) + c^2(\eta) p_T^2 \cdot r_L^4(\eta) + \frac{b^2(\eta) \cdot r_L^2(\eta)}{1 + \frac{d^2(\eta)}{p^2} \cdot \frac{1}{r_L^2(\eta)}}$$

p'_\perp smearing



$$\left(\frac{\sigma_{p'_T}}{p'_T} \right)^2 = a^2(\eta) \cdot r_L^2(\eta) + c^2(\eta) p_T^2 \cdot r_L^4(\eta) + \frac{b^2(\eta) \cdot r_L^2(\eta)}{1 + \frac{d^2(\eta)}{p^2} \cdot \frac{1}{r_L^2(\eta)}}$$

Covariance-enabled fit



- Shape fit in $p_T' \in [30, 50]$ GeV.
- PDF covariance + 300fb^{-1} stat. + smearing included.